10th World Congress on Structural and Multidisciplinary Optimization
May 19 - 24, 2013, Orlando, Florida, USA

Sound vibration damping optimization with application to the design of speakerphone casings

M. Berggren[a], U. Lacis[b], F. Lindström[c], E. Wadbro[a]

[a]Department of Computing Science
Umeå University, Sweden
martin.berggren@cs.umu.se
eddie.wadbro@cs.umu.se

[b]Department of Mechanics
KTH Royal Institute of Technology
Sweden
ugis@mech.kth.se

[c]Limes Audio AB
Sweden
fredric.lindstrom@limesaudio.com

Abstract

We optimize the thickness distribution in a 1D beam model of an elastic plate, subject to forced vibration at one of its ends, in order to minimize the structural vibration in a given area of the plate. The optimization is carried out both in broadband and band-pass cases. Geometric constraints, weight constraints, and constraints on the static compliance are imposed in the optimization. A broadband optimization over 50 frequencies, evenly distributed in the 300–3400 Hz range, reduces the vibration by around 5–10 dB on average throughout the frequency range. When targeting only the higher end of the above frequency range, it is possible to achieve more dramatic results. Vibration reductions of 20 dB and more can be achieved in the 2300–2800 Hz region. In the latter case, the results suggest that a band-gap phenomenon occurs, similarly as for phononic band gap materials. To validate the results, the best-performing optimal shape for the clamped case was imported into a 3D computational structural model, and the resulting forced vibration response agreed well with the the beam-model computations. These results were first announced in a technical report by Lacis et al. [5].

1. Introduction

Speakerphone functionality is used for conference phones, for intercoms, and as a feature in cordless and mobile phones. High quality speakerphones require sophisticated digital signal processing to provide echo cancellation and to reduce feedback. However, the performance of a the digital processing algorithms are often reduced if the device is acoustically not well designed [4]. Special care is needed when the loudspeaker and the microphone are housed in the same cabinet. For instance, damping material such as rubber is then typically deposited at appropriate places. An issue that has received much less attention, however, is how to design the phone casing itself in order to reduce the structural feedback between the loudspeaker and the microphone.

We consider the conceptual configuration illustrated in Fig. 1. The loudspeaker induces lateral vibrations in the casing that will affect the microphone. The question we consider here is how to design the thickness distribution in the region of interest in order to minimize the coupling. Of course, a trivial solution is to cut off the structure completely at some location in the region of interest. To avoid this case, it is therefore necessary to provide conditions that ensure a sufficient static stiffness of the structure.

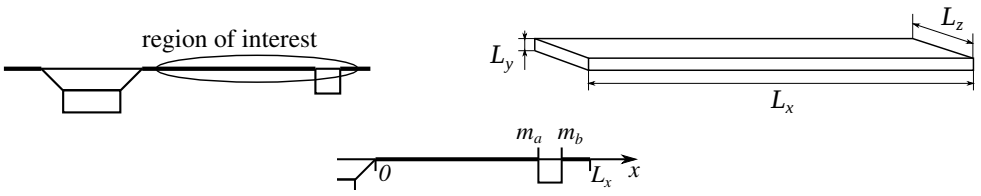

Figure 1: Conceptual configuration of a speaker–microphone configuration (upper left). A plate model of the region of interest (upper right). The microphone is assumed to be located in the area where $\hat{x} \in (m_a, m_b)$ (lower).

We have not found any examples of studies where the thickness distribution of a plate model was optimized for vibration damping. However, previous work of relevance include a study by Yu et al. [9] of the transmission spectrum of a beam with a two-degrees-of-freedom locally resonant structure. The spectral gaps caused by the resonator achieved a measured transmission attenuation of over 20 dB. Christensen et al. [2] provide a review of methods for optimization in the context of coupled structural and acoustics problems, and the same authors also reported on the optimization of sound emission directionality for a baffle-mounted vibrating plate [3]. Sorokin et al [7, 8] addressed the problem of minimizing the vibration energy transfer in structures composed of elastic tubular beams. Decision variables were locations of a few mounting points in the structures. Topology optimization of a 2D elastic continuum was carried out by Olhoff and Du [6] in order to minimize the dynamic compliance subject

to a given time-harmonic excitation. The effect of optimization was generally to move the eigenfrequencies of the optimized structures far from the excitation frequency. They also concluded that an added static compliance condition was beneficial for cases that involved high frequency excitation.

2. Problem formulation

We consider one of the simplest possible models of the region of interest in terms of an elastic thin plate of dimensions L_x, L_y and L_z (Fig. 1). We assume that the thickness of the plate $\hat{\phi}(\hat{x})$ varies in the length ($\hat{x}$) but not in the depth direction ($\hat{z}$). We also assume that all loading conditions are constant in the depth direction and that the plate at the left side is driven with a small time-harmonic shear force $\hat{F}(t) = \hat{F}_0 \mathrm{e}^{-\mathrm{i}\hat{\omega}t}$. The transversal motion of the plate can then be modeled by the following time-harmonic Euler–Bernoulli beam equation for the complex amplitude function $\hat{u}(\hat{x})$:

$$-\rho L_z \hat{\phi}(\hat{x})\hat{\omega}^2\hat{u} + \frac{d^2}{d\hat{x}^2}\left(E\frac{L_z\hat{\phi}^3(\hat{x})}{12}\frac{d^2\hat{u}}{d\hat{x}^2}\right) = 0, \tag{1}$$

were ρ is the mass density of the material and E the Young's modulus. (The ˆ symbol over a variable indicates dimensional quantities in contrast to corresponding nondimensionalized ones introduced below.)

At the right side of the plate, we consider two cases: either a clamped condition or a lossy mounting modeled by a mechanical impedance condition. After appropriate scaling [5], we arrive to the following dimensionless form of the boundary value problem for the (nondimensional) transversal displacement amplitude function $u_\omega(x)$:

$$\begin{aligned} -\omega^2\phi u_\omega + \left(\phi^3 u_\omega''\right)'' &= 0 \qquad \text{in } (0,1),\\ \phi^3 u_\omega''\big|_{x=0} = 0, \qquad \left(\phi^3 u_\omega''\right)'\big|_{x=0} &= F,\\ u_\omega\big|_{x=1} = 0, \qquad u_\omega'\big|_{x=1} &= 0, \end{aligned} \tag{2}$$

for the case of a clamped condition on the right side of the plate, and

$$\begin{aligned} -\omega^2\phi u_\omega + \left(\phi^3 u_\omega''\right)'' &= 0 \qquad \text{in } (0,1),\\ \phi^3 u_\omega''\big|_{x=0} = 0, \qquad \left(\phi^3 u_\omega''\right)'\big|_{x=0} &= F,\\ \phi^3 u_\omega''\big|_{x=1} = 0, \qquad \left(\phi^3 u_\omega''\right)'\big|_{x=1}^{1} &= -\mathrm{i}\omega u_\omega\big|_{x=1}\zeta, \end{aligned} \tag{3}$$

for the case of an impedance boundary condition, where ζ is the (nondimensional) mechanical impedance for the mounting on the right side.

To evaluate the static elastic response $u_0(x)$, we consider the simply supported case with a distributed uniform loading in the transversal direction,

$$\begin{aligned} \left(\phi^3 u_0''\right)'' &= 1 \qquad \text{in } (0,1),\\ u_0\big|_{x=0} = \phi^3 u_0''\big|_{x=0} &= 0,\\ u_0\big|_{x=1} = \phi^3 u_0''\big|_{x=1} &= 0. \end{aligned} \tag{4}$$

We assume that a microphone is mounted on the plate within an interval (m_a, m_b) on the $\hat{x}$ axis (Fig. 1), which after rescaling corresponds to the interval $(a, b) \in (0, 1)$. To measure the vibrations at the microphone location for a given frequency ω of vibration, we choose the objective function

$$J(\phi, u_\omega) = \frac{1}{2}\int_a^b |u_\omega|^2\, dx. \tag{5}$$

The thickness of the plate will be allowed to vary between a strictly positive lower and an upper bound. Moreover, the thickness should be constant in the region of the microphone. We thus choose the following set of feasible thickness distributions:

$$\mathscr{U} = \left\{ \phi \in L^\infty(0,1) \mid 0 < \underline{\phi} \le \phi \le \bar{\phi}, \quad \phi = \phi_0 \text{ in } (a,b) \right\}. \tag{6}$$

Let Ω be the set of frequencies for which we intend to minimize the vibrations in the microphone region. For

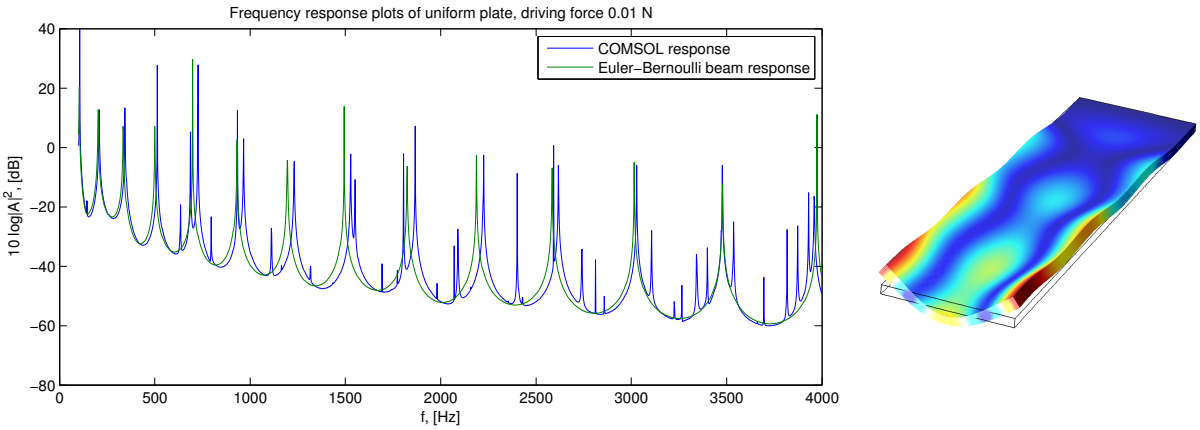

Figure 2: Frequency response for the Euler–Bernoulli beam model and the full 3D model of the plate with uniform thickness (left). Example of a 3D mode that is not modeled by the Euler–Bernoulli beam equation (right).

the case of a clamped right side, the complete optimization problem can now be specified as

$$\begin{aligned}
&\min_{\phi\in\mathscr{U}} \sum_{\omega\in\Omega} \frac{1}{2}\int_a^b |u_\omega|^2\,dx \quad \text{subject to, } \forall\omega\in\Omega,\\
&\quad\begin{cases} -\omega^2\phi u_\omega + \left(\phi^3 u_\omega''\right)'' = 0 & \text{in } (0,1),\\ \phi^3 u_\omega''\big|_{x=0} = 0, \qquad \left(\phi^3 u_\omega''\right)'\big|_{x=0} = F,\\ u_\omega\big|_{x=1} = 0, \qquad u_\omega'\big|_{x=1} = 0, \end{cases}\\
&\int_0^1 \phi\,dx \le \gamma_m, \qquad \int_0^1 u_0\,dx \le \gamma_c C_{\text{ref}}, \quad \text{where}\\
&\quad\begin{cases} \left(\phi^3 u_0''\right)'' = 1 & \text{in } (0,1),\\ u_0\big|_{x=0} = \phi^3 u_0''\big|_{x=0} = 0,\\ u_0\big|_{x=1} = \phi^3 u_0''\big|_{x=1} = 0, \end{cases}
\end{aligned} \tag{7}$$

in which γ_m constitutes a mass constraint and γ_c the static compliance constraint with respect to a reference compliance C_{ref}. In the case of an impedance boundary condition to the right, the state equation for u_ω above should be replaced by equation (3). Finite-element solutions of state equations (2) (or (3)) and (4) are implemented in a standard way using cubic Hermite elements on a uniform mesh, where the thickness distribution ϕ in the discrete case is constant on each interval.

3. Parameter values

We choose parameter values of relevance for a conference phone. The chosen plate dimensions are

$$L_x = 0.280\text{m}, \quad L_z = 0.070\text{ m}, \quad L_y = 0.005\text{ m}. \tag{8}$$

We also use

$$\rho = 1.1\text{ g/cm}^3, \quad E = 360\text{MPa}, \tag{9}$$

which correspond to (a rather weak) ABS plastic. For the 3D simulation validations reported below, the Poisson ratio is $\nu = 0.35$. The mechanical impedance in (3) was set to $\zeta = 10$, a value that was empirically decided in order to obtain a moderate damping of the frequency response.

We will optimize the response of the plate for frequencies in the band $\omega \in 2\pi(300, 3400)$ s^{-1}, which is a traditional frequency band considered in telephony.

4. Model validation

To validate our simple beam model of the vibrating plate, we compared the frequency response of our beam model with corresponding 3D response calculated in Comsol Multiphysics. As shown in Fig. 2, the agreement is overall good. The excess peaks for the 3D model are oscillation modes (such as the one shown to the right in Fig. 2) that are not modeled by the Euler–Bernoulli beam equation.

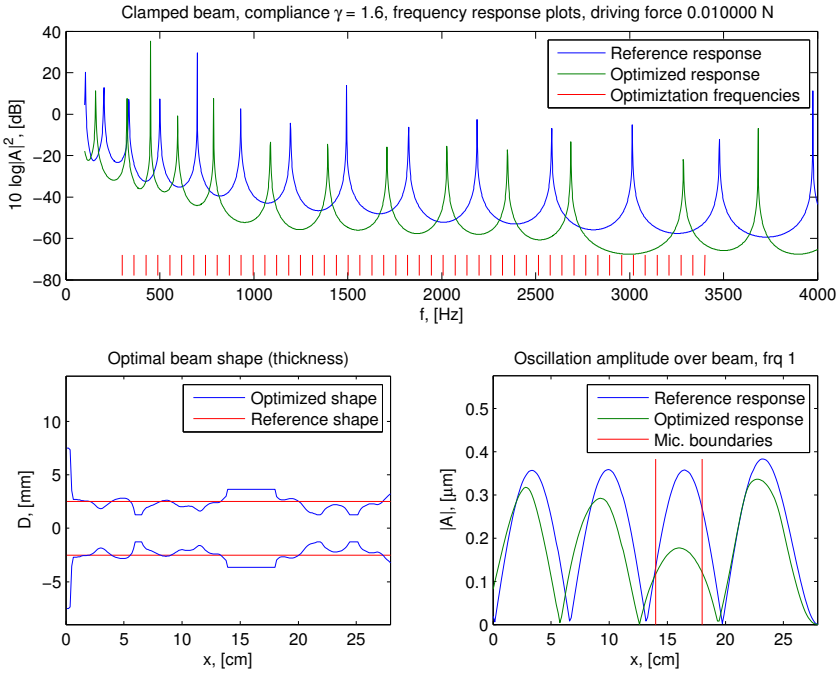

Figure 3: Results from a broad band optimization for the clamped plate. The frequency response, the optimal shape, and the vibration response for the lowest optimization frequency is shown.

5. Results

The discrete version of optimization problem (7) is solved using fmincon from Matlab's optimization toolbox, which implements a Sequential Quadratic Programming method. Gradients of the objective function are computed by solving associated adjoint equation, and a standard sensitivity analysis yields similarly also the gradient of the static compliance. A uniform-thickness plate serves as the reference shape, whose mass constitutes mass constraint γ_m. The compliance of the reference shape, calculated from corresponding solution of equation (4), constitutes C_{ref} in problem statement (7), and we choose $\gamma_c = 1.60$; that is, the static compliance is allowed to increase by 60 % after optimization. The (nondimensional) mesh size is $h = 10^{-2}$.

5.1. Broad band optimization

As a first case study, the whole telephony band $I_{\text{BB}} = 2\pi\,(300, 3400)$ Hz is selected for optimization. Fifty equally spaced frequencies in the interval I_{BB} are selected as the frequency set Ω in problem (7). A result of the optimization is shown in Fig. 3 for the case of a clamped right side boundary condition and in Fig. 4 for the lossy impedance condition. Various different constraint configurations were tested and yielded conceptually similar results.

5.2. Pass band optimization

For the next case studies, we considered six 500 Hz frequency windows $I_n = 2\pi\,(300 + 500n, 800 + 500n)$ Hz with $n = 0, \ldots, 5$. In each window, fifty equally spaced frequencies are selected as the frequency set Ω. Example results for low and high frequency windows are shown in Fig. 5 and Fig. 6, respectively, for the case of a clamped boundary condition on the right side. In this case, the optimization displayed a tendency to develop irregular shapes, which is why we here included a design filter in the optimization formulation. The filter is a 1D analogue of a kind of filter that is routinely applied in topology optimization of elastic structures [1, p. 35–36]. The filter radius was around 4×10^{-2} (nondimensional) and was adapted heuristically to obtain sufficient smoothing of the shapes. The better-performing beam shape (Fig. 6) was imported into Comsol Multiphysics for validation in a 3D dynamics simulation of the frequency response. The thickness distribution in correct proportions is shown in Fig. 8, and Fig. 9 shows a perspective picture of the plate. The frequency response plots from the Comsol simulations are shown in Fig. 7, which compares well with corresponding 1D result in Fig. 6.

The same case studies were repeated for the case of an impedance boundary condition on the right side. An example result of a high frequency window optimization is shown in Fig. 10.

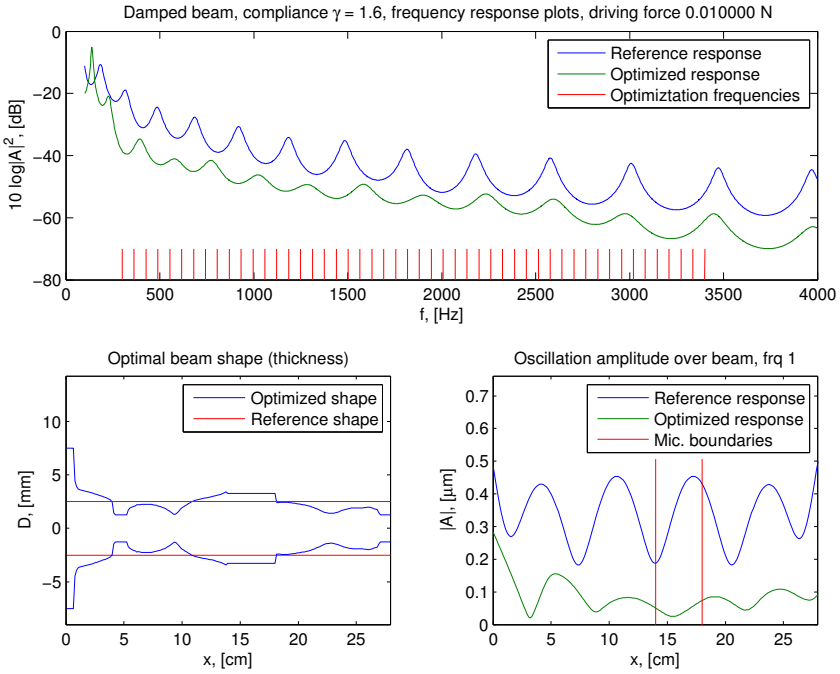

Figure 4: Results from a broad band optimization for the damped beam. The frequency response, the optimal beam shape, and the vibration response over the beam for the lowest optimization frequency is shown.

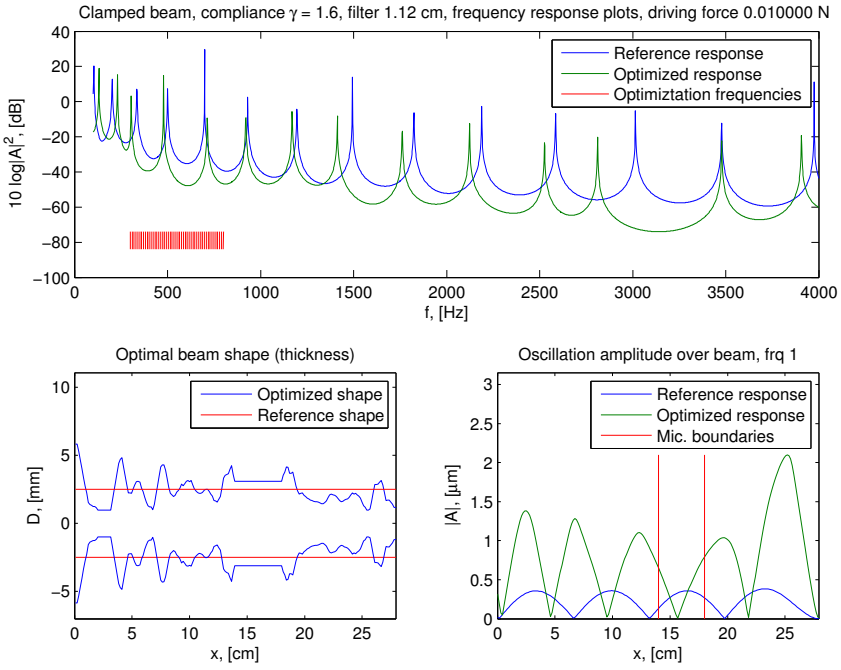

Figure 5: An example frequency window $(300, 800)$ Hz optimization result for clamped beam. The frequency response, the optimal beam shape, and the vibration response over the beam for the lowest optimization frequency is shown.

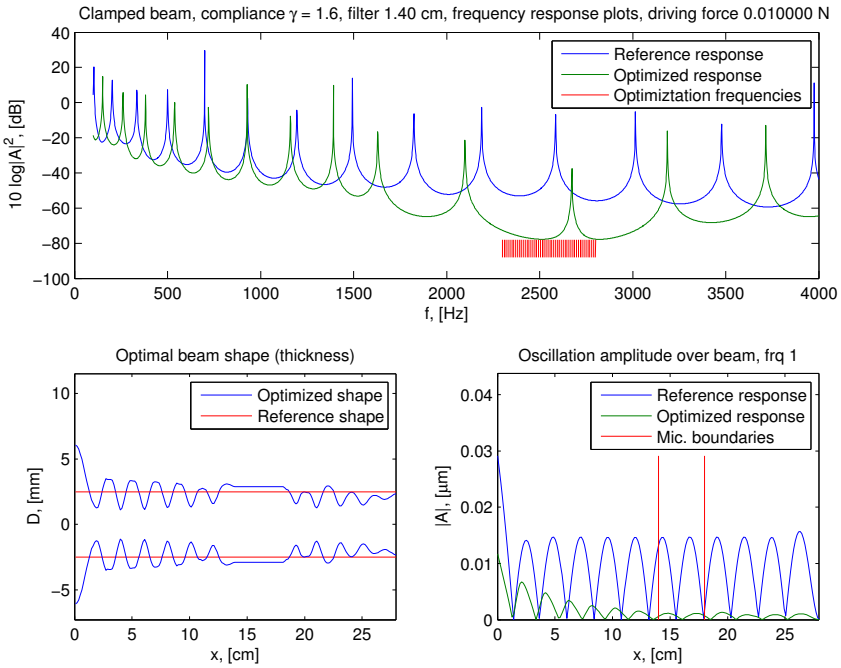

Figure 6: An example frequency window $(2300, 2800)$ Hz optimization result for clamped beam. The frequency response, the optimal beam shape, and the vibration response over the beam for the lowest optimization frequency is shown.

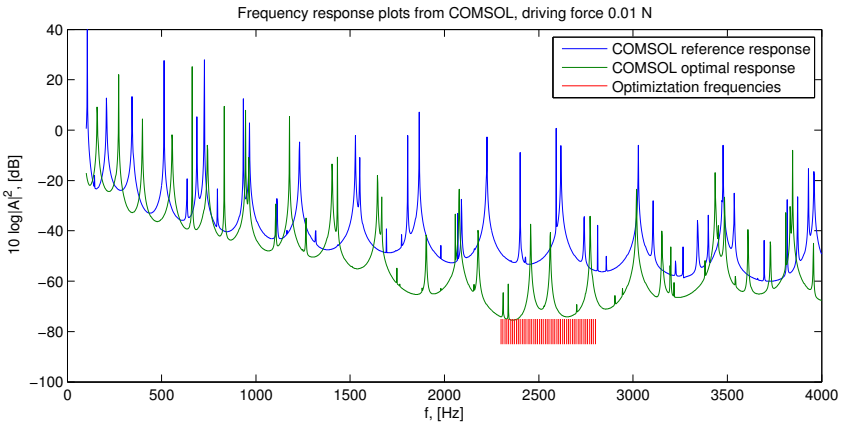

Figure 7: A 3D validation of the optimal beam shape for frequency window 4 (cf. Fig. 6). The frequency response results from the Comsol Multiphysics simulations are shown.

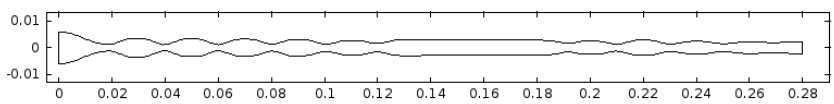

Figure 8: The optimal beam shape (see Fig. 6) in correct proportions, as imported into Comsol Multiphysics.

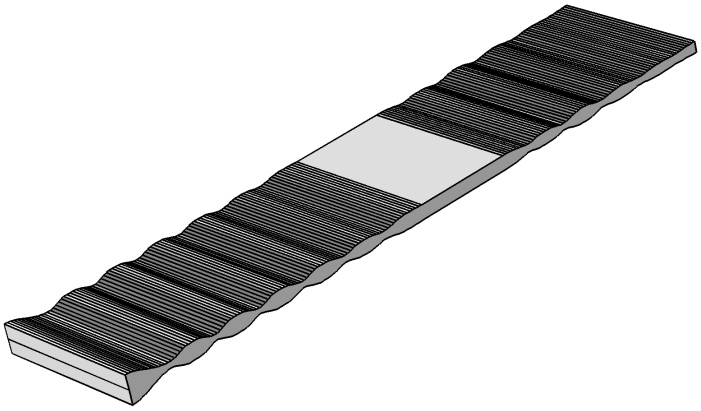

Figure 9: Perspective picture of the optimal plate as imported into Comsol Multiphysics.

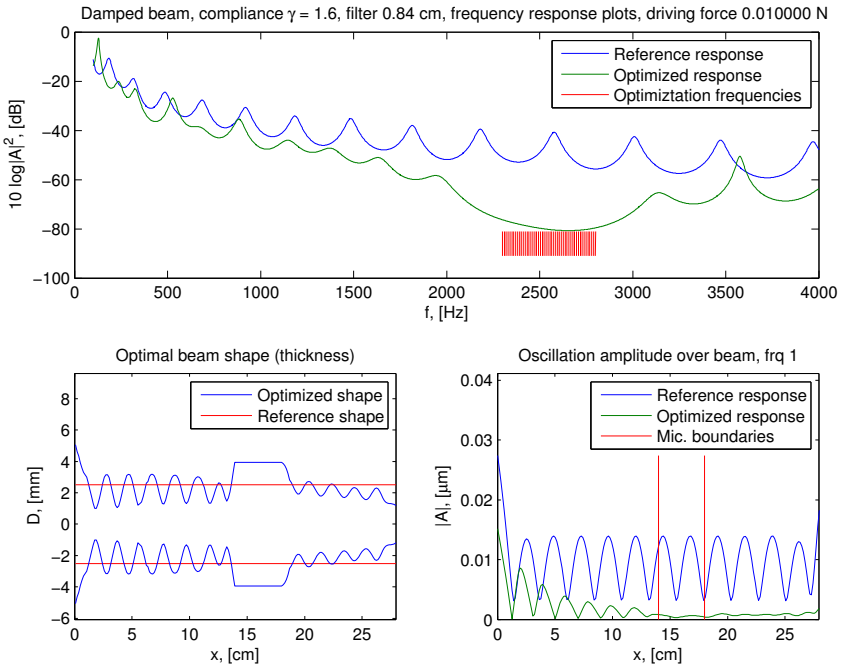

Figure 10: An example frequency window $(2300, 2800)$ Hz optimization result for damped beam. The frequency response, the optimal beam shape, and the vibration response over the beam for the lowest optimization frequency is shown.

6. Discussion

The vibration response of the 1D beam model that we use matches well the response from a full 3D model, as was confirmed both for the initial plate of uniform thickness as well as for one of the optimized shapes. The obvious advantage of using the 1D model is the low computational cost, which allowed the treatment of a somewhat involved optimization formulation with multiple frequencies and static constraints, and allowed a thorough investigation of a large number of cases besides those shown here.

The results demonstrate that it is possible in many cases to obtain significant reductions of the vibrations in the microphone region by redistributing the material of a uniformly thick plate. The least improvements were obtained when targeting solely the low end of the spectrum. Better overall results was possible to achieve in the broad band case, where roughly a 5–10 dB damping of the vibrations was achieved. The best improvements were obtained when targeting the high end of the spectrum, where roughly a 20 dB damping was achieved. An important part of the mechanism that causes the damping is a thickening of the plate around the source and sometimes also around the microphone. Such a design is likely to cause less energy to be extracted from the source. The perhaps most intriguing result was the pass band cases at the higher frequencies, where a band-gap phenomenon appears to occur. The optimization procedure produces quasi-periodic shapes with a period similar in size to the structural wave length for the considered frequencies (Figs.6 and 10). The structures resemble those occurring in phononic band gap materials [1, pp. 138–148].

References

[1] M. P. Bendsoe and O. Sigmund. *Topology Optimization. Theory, Methods, and Applications*. Springer, 2003.

[2] S. T. Christensen, S. V. Sorokin, and N. Olhoff. On analysis and optimization in structural acoustics — part I: Problem formulation and solution techniques. *Struct. Opt.*, 16:83–95, 1998.

[3] S. T. Christensen, S. V. Sorokin, and N. Olhoff. On analysis and optimization in structural acoustics — part II: Exemplifications for axisymmetric structures. *Struct. Opt.*, 16:96–107, 1998.

[4] E. Hänsler and G. Schmidt. *Acoustic Echo and Noice Control: A Practical Approach*. Wiley, 2005.

[5] U. Lacis, E. Wadbro, and M. Berggren. Design optimization of phone casings for sound vibration damping: preliminary studies on the Euler–Bernoulli beam model. Technical Report UMINF 12.16, Department of Computing Science, Umeå University, 2012.

[6] N. Olhoff and J. Du. Topological design of continuum structures subjected to forced vibration. In J. Herskovits, S. Mazorche, and A. Canelas, editors, *6th World Congress on Structural and Multidisciplinary Optimization*, 2005. Paper 1701.

[7] S. V. Sorokin, J. B. Nielsen, and N. Olhoff. Analysis and optimization of energy flows in structures composed of beam elements — part I: problem formulation and solution techniqes. *Struct. Multidiscip. Optim.*, 22:3–11, 2001.

[8] S. V. Sorokin, J. B. Nielsen, and N. Olhoff. Analysis and optimization of energy flows in structures composed of beam elements — part II: examples and discussion. *Struct. Multidiscip. Optim.*, 22:12–23, 2001.

[9] D. Yu, Y. Liu, H. Zhao, G. Wang, and J. Qiu. Flexural vibration gaps in Euler–Bernoulli beams with locally resonant structures with two degrees of freedom. *Phys. Rev. B*, 73(064301):1–5, 2006.